Is the Galactic Center Source, IRS 21, as Large as It Appears?

A. M. Tanner[a], A. M. Ghez[a], M. Morris[a], E. E. Becklin[a], A. Cotera[b], M. Ressler[c]

[a]UCLA Department of Astronomy and Physics, Los Angeles, CA 90095
[b]AMES/SETI
[c]JPL

ABSTRACT

We present diffraction limited 2-25 μm images, obtained with the W. M. Keck 10-m telescopes that spatially resolve the cool Galactic Center source IRS 21, an enigmatic object that has alluded classification. Modeled as a gaussian, the azimuthally averaged intensity profile of IRS 21 has a HWHM radius of 740±30 AU at 2.2 μm and an average HWHM radius of 1540±90 AU at mid-infrared wavelengths. These sizes along with its color temperature favor the hypothesis that IRS 21 is self-luminous rather than an externally heated dust clump. Based on the size alone, the remaining possible dust geometries are (1) an intrinsic inflow or outflow or (2) an extrinsic dust distribution, in which case IRS 21 could be simply embedded in the Northern Arm. A simple SED model of the infrared photometry from the literature and our mid-infrared images reveal that the near-infrared radiation is scattered light from an unknown embedded source while the mid-infrared radiation is the remaining re-radiated light. The agreement between the 2.2 μm polarization angle for IRS 21 and the 12.5 μm polarization angle at the position of IRS 21 ($\phi_{2.2}$-$\phi_{12.5}$=23±17.0), the symmetric shape of its intensity profiles, as well as the similarity of the observed properties of all the Northern Arm sources, lead us to conclude that the scattering dust around IRS 21 is extrinsic to the central source and is associated with the Northern Arm.

Keywords: Infrared: stars, dust; Galactic Center: IRS 21, Sgr A*, Northern Arm

1. INTRODUCTION

IRS 21 is one of the more unusual objects in the central parsec of our Galaxy. It has the largest K band polarization ($\sim$10%[1,2]) , and is one of only two objects (IRS 21 and IRS 1W) to have both an H-K color >3[3] and a featureless K band spectrum.[4] Gezari et al.[5] initially identified IRS 21 in 8.3 and 12.4 μm images as a strong mid-infrared peak located along the Northern Arm, a tidal stream of dust and gas that is infalling towards and orbiting around the supermassive (M_{BH} = 2.6×10^6 M$_\odot$[6]) central black hole, and suggested that it is an externally heated, high density dust clump.[5,7] However, a variety of other classifications have also been proposed, including an embedded early-type star,[4] and a young stellar object (YSO).[3]

In this proceeding, we present the spatially resolved structure of IRS 21 at near- and mid-infrared wavelengths, based on diffraction limited imaging at the W.M. Keck 10-m telescopes. At the distance to the Galactic Center, 8 kpc,[8] the angular resolution of these images ranges from 400 AU at 2.2 μm to 3370 AU at 24.5 μm. We use the derived spatial and photometric information, combined with polarization measurements from the literature, to constrain the nature of this enigmatic object.

2. OBSERVATIONS

IRS 21 was observed in the K (2.2 μm) bandpass using the Keck I 10-meter telescope and the facility near-infrared camera (NIRC)[9,10] on the nights of 1995 June 10-12, 1996 June 26-27, 1997 May 13, 1998 April 2, 1998 May 14-15, 1998 August 4-6, 1999 May 2-4 and 1999 July 24-25. During these observations, the long-exposure seeing at 2.2 μm was on average $\sim$0.6". While the majority of the images were obtained for a proper motion study of the central stellar cluster [6] and were, therefore, centered roughly on the nominal position of Sgr A* (3" away from IRS 21), some images taken in 1998 August were centered approximately on IRS 21. Each observation consisted of several sets of short exposure (t_{int} = 0.15 sec) frames, which freeze the distortion introduced by turbulence in the Earth's atmosphere. The resulting speckle frames, which have a pixel scale of 0.02"/pixel and a corresponding field of view of 5"×5", contain high spatial resolution information that is recovered in post-processing.

Diffraction-limited images were obtained from the speckle frames as described by Ghez et al.[6] and briefly summarized here. The individual frames were calibrated in the standard manner: bad-pixel-corrected, sky-subtracted and flat-fielded. The frames were combined in sets of $\sim$100, by shifting on the brightest speckle of a nearby point source (IRS 16C or IRS 33E) to generate the shift-and-add (SAA) images. The resulting SAA point spread function (PSF) consists of a seeing halo and a diffraction limited core (FWHM of 0.05") containing $\sim$10% of the total light.

Mid-infrared images of IRS 21 were obtained through narrow band filters ($\frac{\Delta\lambda}{\lambda} \sim$0.1) at 8.8, 12.5, 20.8, and 24.5 μm with the MIRLIN[11] mid-infrared camera mounted on the Keck II 10-meter telescope. The 8.8 and 24.5 μm data were collected in 1998 March while the 12.5 and 20.8 μm data were collected in 1998 June. These images have a plate scale of 0.15"/pixel over an instantaneous field of view of 7"X7". The chop-nod pairs were double differenced, airmass calibrated, sub-pixellated by a factor of 3 and registered to create a $\sim$25"×25" mosaic of a region centered on Sgr A* including IRS 21.

3. RESULTS

3.1. Near-Infrared Size

IRS 21's remarkable extent is evident in Figure 1, which contrasts the raw SAA 2.2 μm images of IRS 21 and the point source, IRS 33E. Ott et al.[1] present lower spatial resolution (θ_{res}=0.15") images indicating that IRS 21 is extended; however, they do not report a size estimate. The image of IRS 21 shows no obvious deviation from circular symmetry. Therefore, our analysis of its size is performed in one dimension by comparing the azimuthally-averaged intensity profile of IRS 21 with that of the PSF. Due to their isolated positions within the image, IRS 16NE is used as the PSF for all of the central cluster images while IRS 33E is used as the PSF for those images having IRS 21 centered in the field of view. Since the source density in this region is large, an area 0.6" in radius around any neighboring sources brighter than $m_k \sim$14 is excluded from the azimuthal averages. Each pixel included in the average is weighted by the number of frames that contributed to its value in the SAA processing. The background is subtracted based on the median value of the radial profile between 1.0" and 1.1". Figure 2a shows an example of the resulting radial profiles for IRS 21 and a PSF with error bars which represent the standard deviation of the mean intensity at each radius.

Once the intensity profiles are extracted, an intrinsic size is estimated by modeling the observed IRS 21 profile as the convolution of the normalized PSF profile with a Gaussian function. Figure 2a also shows the best fitting model profile (dashed line), from which we use the Gaussian HWHM to estimate a radius of IRS 21 for each SAA image. Table 1 lists the average radius and standard deviation from all epochs of data. The 2.2 μm radius appears to have remained constant from 1995 to 1999, with an average value of 740±30 AU.
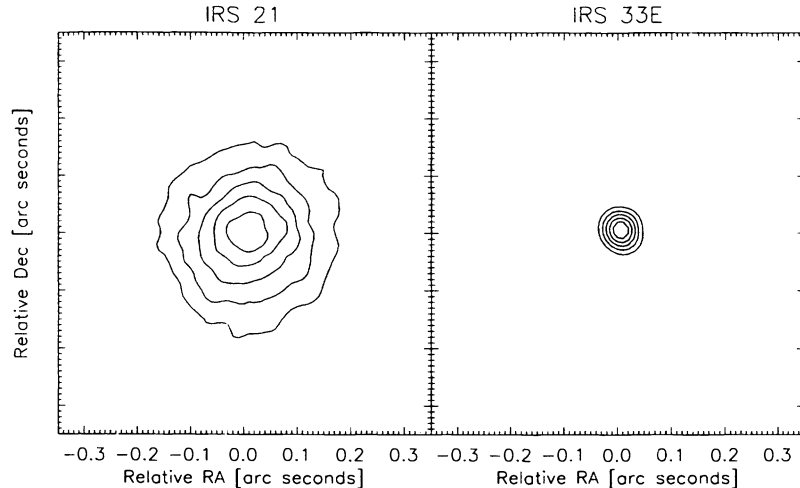
Figure 1. The contours of IRS 21 from a raw Shift and Add (SAA) 2.2 μm image are plotted showing the extended nature of IRS 21 compared to its neighboring point source, IRS 33. The contours plotted for IRS 21 and IRS 33E represent 90-50% of the peak value in 10% increments.

3.2. Mid-Infrared Size and Flux Densities

IRS 21 is also clearly extended in all of the mid-infrared MIRLIN images (see Figure 2), however the structure of the diffuse background emission from the Northern Arm complicates the analysis. We use the CLEAN algorithm to separate IRS 21 from the Northern Arm diffuse emission. IRS 3, a bright and isolated mid-infrared source, is marginally extended at 8.8 μm and appreciably extended at 12.5, 20.8 and 24.5 μm requiring a separately observed PSF standard star (i.e. β Leo, α Bootes, or α Scorpius) to be used. A model of the diffuse emission is created by applying the CLEAN algorithm to an area 0.7″ in radius around IRS 21, effectively removing it from the image. The cleaning process is halted when the RMS of the residual map compared to an inclined plane that was matched to the background prior to cleaning, begins to increase. Figure 3 shows the results of subtracting the estimate of the Northern Arm diffuse emission (the residual map) from the original image.

The background subtracted image is then used to create an azimuthally-averaged radial intensity profile which is analyzed similarly to the near-infrared radial profile (see Figure 2b). To correct for any seeing affects, the 8.8 μm size was estimated using the sizes resulting from both IRS 3 and β Leo as the PSF. Table 1 lists the mid-infrared radii and their errors. Table 1 also lists the mid-infrared fluxes measured for IRS 21 by comparing the total counts within the background subtracted image to the infinite-aperature-corrected counts within a 20 pixel (1″) radius aperture around the PSF standard star.

4. DISCUSSION

The immense size of IRS 21 at 2.2 μm and in the mid-infrared is well beyond that expected for a stellar photosphere by a minimum of two orders of magnitude. For comparison, the radius of the largest stellar photosphere, an M supergiant, is roughly 4 AU. We are, therefore, most likely detecting a dust photosphere. In the following subsections, we consider the origin of the dust photosphere (4.1), the physical process giving rise to the observed 2.2 μm light (4.2), and the nature of the underlying source (4.3).
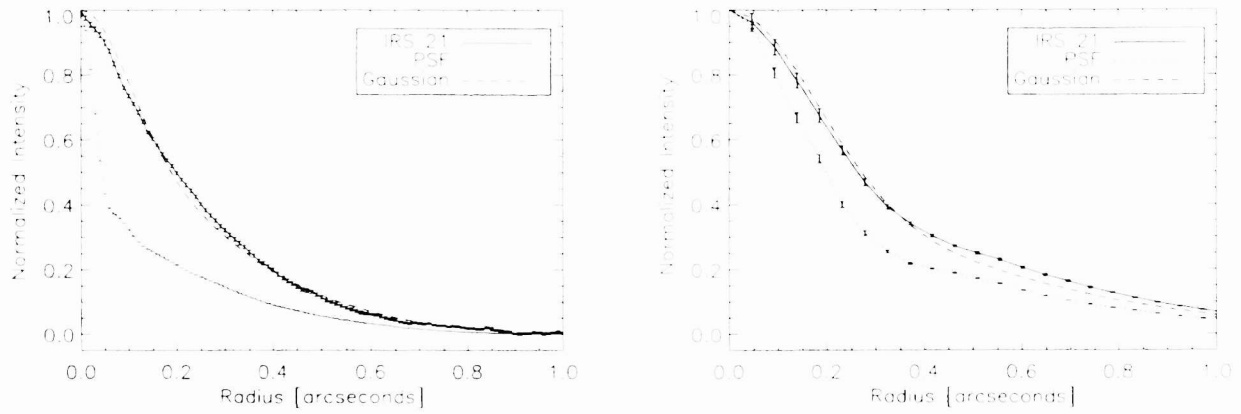
Figure 2. a) Radial profiles of the background subtracted images of IRS 21 (solid line) and a PSF star (dotted line) along with the profile of the convolution of the PSF with a Gaussian (dashed line) (a) at 2.2 μm and (b) at 12.5 μm.
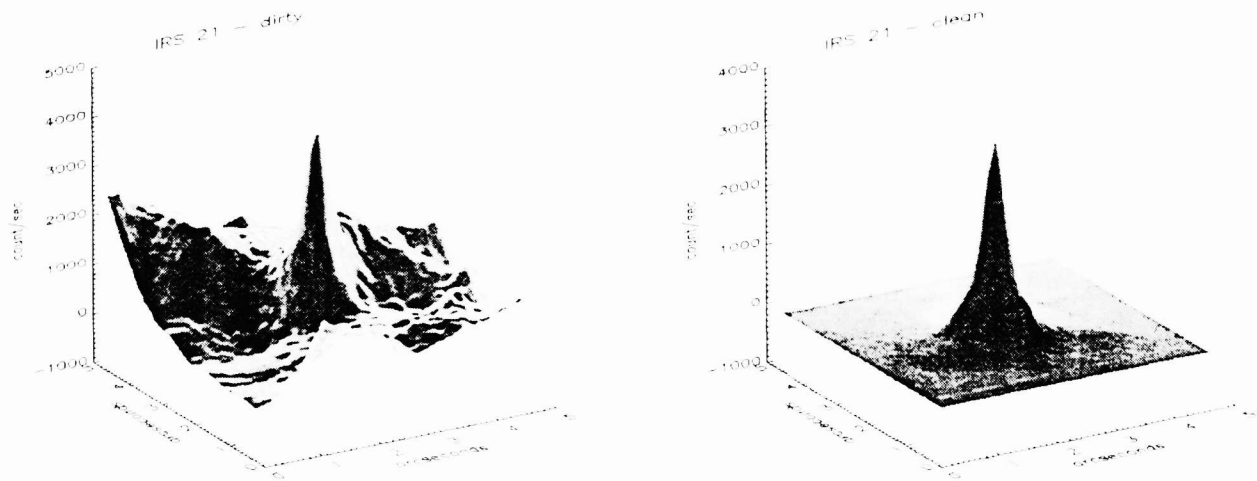

Figure 3. A comparison of the raw MIRLIN 12.5 μm image of IRS 21 to the background subtracted image (see text for discussion of background estimate).

Table 1. Near- and Mid-infrared Radius and Flux of IRS 21

λ	Flux [Jy]	Radius [AU]
2.2	0.05 ± 0.002^3	740 ± 30
8.8	4.24 ± 0.2	1540 ± 210
12.5	8.5 ± 0.83	1575 ± 175
20.8	4.28 ± 0.8	1400 ± 410
24.5	3.34 ± 0.033	1560 ± 120

4.1. Origin of the Dust Photosphere: Extrinsic versus Intrinsic to the Central Source

While IRS 21 was originally classified as a dust clump externally heated by the hot stars in the IRS 16 cluster,[5] its color temperature in our MIRLIN 12.5/20.8 μm map is hotter than that of the surrounding Northern Arm dust, suggesting it is self-luminous.[12] There are then two possibilities for the origin of the large observed dust sizes, it could be either intrinsic or extrinsic to the central radiative source. The intrinsic case is interesting because of the tidal field of the nearby supermassive black hole. Dust which is intrinsic to the star could be associated with either an inflow or outflow of material from a central stellar object. The Roche limit for a star of mass, M, at the projected distance of IRS 21 from Sgr A* is 480 AU $(M/10~M_\odot)^{1/3}$, which is comparable to its measured size. So in principle, the near-infrared emitting dust could be bound to the star but only marginally, and only if the star is relatively massive. However, no known outflow source has an observed 2.2 μm radius comparable to the 740 AU observed for IRS 21. For instance, the well-studied carbon star IRC +10216, whose dust shell is optically thick at 2.2 μm, has an estimated radius of $\sim$ 50 AU.[13] Other examples of the largest observed dust photospheres at 2.2 μm include the spiral dust shell around the binary Wolf-Rayet star, WR 104, and the dust shell around the Wolf-Rayet star, Ve 2-45, which have diameters 160 AU and 70 AU. respectively.[14,15] The alternative to an intrinsic dust shell would be that the observed dust is extrinsic to the central source, in which case we are simply observing the object embedded in the Northern Arm.

One piece of evidence which may distinguish between the intrinsic and extrinsic dust scenarios comes from polarization measurements. Aitken et al.[16] report polarized 12.5 μm light at the position of IRS 21 with strength $7.5\pm1.2\%$ and a position angle of -9 ± 14°. This appears to be part of a large-scale pattern attributed to polarized thermal emission from dust grains aligned by the magnetic field within the Northern Arm. With a beam size of 1", Aitken et al.[16] did not distinguish IRS 21 as a discrete polarization source above the extended flux of the Northern Arm. Therefore, this mid-infrared polarization measurement is dominated by the Northern Arm background and is consequently a measure of the Northern Arm dust properties alone. Any contribution from IRS 21 to the strength or the orientation of the polarization at this wavelength is apparently diluted to insignificance. In contrast, at 2.2 μm, IRS 21 is clearly detected as a distinct source of highly polarized light with strength $9.8\pm1.3\%$ at position angle 14 ± 10°.[1] This measurement provides a direct probe of the dust photosphere that is spatially resolved in the observations presented here. The similarity between the orientations of the 2.2 and 12.5 μm polarization vectors, which differ by only 23 ± 17° implies that the dust responsible for each wavelength's emission has the same orientation, if the 2.2 μm polarization is owed to scattering or thermal emission, and not to absorption. Since it is unlikely that grains in an intrinsic dust shell would be aligned by the large scale magnetic field in the Northern Arm, such a co-alignment suggests that the observed 2.2 μm dust photosphere is part of the Northern Arm and is not intrinsic to the source.

However, the uncertainties in the position angle are sufficiently large to imply that even randomly

oriented vectors would appear to be aligned within the 2σ uncertainties $\sim$20% of the time. This requires us to consider the possibility that the alignment of the 2.2 and 12.5 μm polarization vectors is coincidental. In this case, if an intrinsic dust shell is responsible for the 2.2 μm polarized light, it would require that the dust distribution have a pronounced asymmetry in order to produce the large degree of 2.2 μm polarization. Without such an asymmetry, the dust shell might require, for example, an azimuthally asymmetric magnetic field strong enough to align dust grains on the relatively short time scales (few $\times 10^3$ years) of the outflow, which is unlikely. Therefore, since no such asymmetry is observed at our resolution of 0.05'' (see Figure 1), we conclude that the dust is unlikely to be intrinsic to the central star.

Finally, the presence of an unusually large concentration of luminous stars in the Northern Arm having characteristics similar to those of IRS 21 is also supportive of the hypothesis that the environment of the Northern Arm is itself responsible for the extended nature of IRS 21 and its SED. Most of the most prominent mid-infrared sources in the central parsec are distributed along the Northern Arm (IRS 1, 10, 5 and 8) (e.g. Becklin et al.[17]). This point will be revisited in a later publication.

4.2. Spectral Energy Distribution and Model

The 2.2 μm light is either scattered or thermally reprocessed by dust located $\sim$740 AU away from the central source. One possible interpretation is emission from shock heated dust which is not in radiative equilibrium.[18] However, this emission model does not reproduce the large observed H-K color (see Figure 4). In addition, the observed featureless spectrum rules out H_2 fluorescence as a source of near-infrared emission. To understand the nature of the near- and mid-infrared emission, we have constructed a spectral energy distribution (SED) for IRS 21 using photometry collected from the literature, calibrated assuming zero points from Tokunaga,[19] as well as the fluxes listed in Table 1. The ISM extinction law, which affects both the near- and mid-infrared flux, is derived from the mid-infrared silicate extinction coefficients of Laor and Draine[20] and the observed near-infrared extinction law of Rieke, Rieke and Paul.[21] The shape of the SED suggests there are two distinct emission components: one in the near-infrared responsible for the flux between 2-4 μm, and a separate, mid-infrared component.

To utilize both the spectral and spatial information, we created a simple radiative transfer model which provides an SED and a line-of-sight intensity profile. The dust is assumed to be in a shell with a thickness, dr, inner radius, r_i, and radial gas density, $n_H(r)$, with an inverse power-law index of 0, 1 or 2 where a $1/r^2$ density fall off is indicative of mass loss. The near-infrared SED component is modeled by a central source of blackbody emission (optically thick dust) extincted by the inner portions of the shell and then singlely scattered at a distance, r. The scattering, which is assumed to be isotropic, is essential to account for the large observed J-K color. The mid-infrared SED component is modeled as re-emission by silicate dust grains whose temperature is determined through radiative equilibrium, dependent on the radius and temperature (r_{cen} and T_{cen}) of the central source and its distance to the dust. The emission and scattering coefficients for the silicate dust are derived from the silicate grain coefficients of Laor and Draine.[20] The dust grain size distribution is modeled assuming a Mathis, Rumpl, and Nordsieck (1977, MRN), power-law ($dn/da \propto a^{-3.5}$) with radii ranging from 0.005 to 0.25 μm. An array of scattering and re-emission spectra are estimated as a function of radius through the dust shell. The total flux, as a function of separation from the central source on the plane of the sky, is estimated by integrating along the line of sight while accounting for additional extinction through the remaining dust shell.

A unique solution to the model SED was found by minimizing the χ^2 value for the fit to the near (1.6-4.7 μm) and mid-infrared (7.8-24.5 μm) photometry. It is not possible to fit the SED using the same dust grain population for both the scattering and re-emission spectra due to a lack of near-infrared emission compared to that in the mid-infrared for a single population. Hence, the mid-infrared emission and near-infrared scattering optical depths are considered as two separate free parameters. The intrinsic
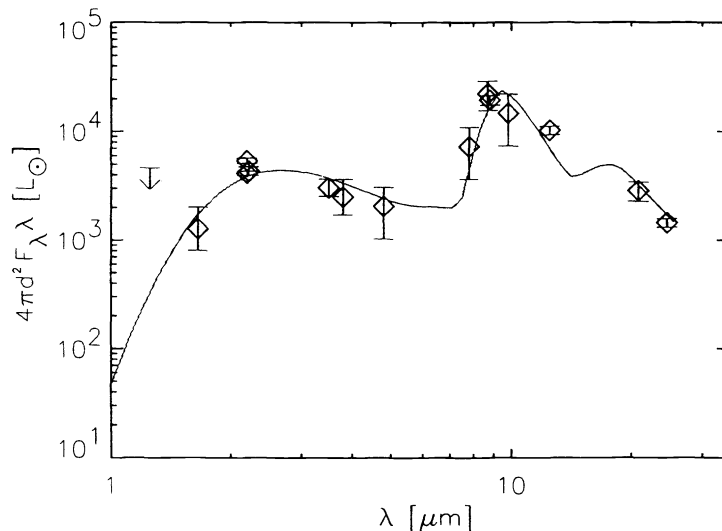
Figure 4. Photometry and the best fitting radiative transfer model for IRS 21 are plotted and show the two components of near-infrared scattered light and mid-infrared re-emitted light. References: J (1.25 μm)[3]; H (1.6 μm), M. Rieke, private com.; K (2.2 μm)[3,24,25]; L (3.5 μm)[23]; L' (3.8 μm)[26]; 8.7 μm,[7] D. Gezari, private com.; 12.4 μm, D. Gezari, private com.; 8.8, 12.5, 20.8 and 24.5 μm, this work

dust extinction optical depth is then related to the scattering optical depth through the albedo. The five parameters (T_{cen}, r_{cen}, r_i, τ_{scat}, and τ_{em}) are varied over a broad range while the Powell minimization algorithm is used to find the minimum χ^2 solution. The shell thickness is constrained by the observed near-infrared azimuthally averaged intensity profile (see Section 3.1). The errors for the free parameters are estimated from the standard deviation of the best fitting values using the three choices for the gas density power-law index.

The SED model with the overall minimum χ^2 value has a dust temperature of 400±40 K at an inner radius of 620±140 AU. The temperature and size of the central source are 570±50 K and 215±70 AU, respectively, indicative of a large central dust photosphere. Since the source of the near-infrared light is modeled as a blackbody, its temperature and radius provide an estimate for the luminosity of 5×10^5 L$_\odot$. The scattering and emission optical depths are dependent on the assumed thickness of the dust shell which must be $\sim$2000 AU to reproduce the extended near-infrared intensity profile. For this shell thickness, the scattering optical depth at 2.2 μm and the emission optical depth at 8.8 μm are $2.5 \pm 2 \times 10^{-5}$ and $2 \pm 0.6 \times 10^{-6}$, respectively. These low optical depths suggest a gas density at the inner radius of 10^2-10^3 cm^{-3} which is smaller than the expected Galactic Center value of 10^5cm^{-3}.[22] The best fitting SEDs require a wide range of ISM extinction corrections (A_V=25±10), however whether any extinction in addition to the typical value of A_V=30 mag for the Galactic Center[21] is due to the ISM along the line of sight or within the dust associated with IRS 21 remains unclear. Since the narrow shape of the near-infrared radial intensity profile suggests an absence of a peak in the flux expected at the inner dust radius of an optically thin dust shell, it is possible that the dust geometry is more consistent with a layer of material as expected for dust associated with the Northern Arm.

4.3. Nature of the Underlying Source

Because the near-infrared light is featureless, it is probably created at an embedded dust photosphere, about which we have little information, and which itself hides the central star. The only information we have on the central star is a crude estimate of its luminosity ($L \sim 5 \times 10^5$ $L_\odot$) and size (~ 200 AU), which still allows for several possibilities: a massive main-sequence star ($M > 10$ $M_\odot$), a massive post-main sequence star, or and AGB star. Inasmuch as these alternatives can be differentiated by the properties of their winds, they can perhaps be distinguished using spectroscopic shock diagnostics in the mid- and far-infrared, where the opacity is not prohibitive. Deeper spectroscopic observations with high spatial resolution at K would also be worthwhile, with the goal of finding the obscured spectroscopic signature of the stellar photosphere or wind.

5. CONCLUSION

The near- and mid-infrared light from IRS 21, a luminous star at the Galactic Center, has been resolved, giving a remarkably large radius of 740-1540 AU. Using current information on the spectral energy distribution and the near and mid-infrared polarization in this direction, we interpret this size in terms of the fact that IRS 21 is embedded in the dense "Northern Arm" component of Sgr A* West, and that the obscured starlight is diffusing out through the optically thin dust in this feature. The obscured near-infrared light is therefore scattered light which probably originated in a dust photosphere overlying the central star. IRS 21 may serve as a prototype for several other extended stars lying along the Northern Arm, including IRS 1W, 10W, 5 and 8.

ACKNOWLEDGMENTS

REFERENCES

1. Ott, T., Eckart, A., & Genzel, R., 1999, ApJ, 523, 248
2. Eckart, A., Genzel, R. Hofmann, R., Sams, B.J., and Tacconi-Garman, L.,E., 1995, ApJ, 445, L23
3. Blum, R. D., Sellgren, K., & DePoy, D. L. 1996, ApJ, 470, 597
4. Krabbe et al., 1995, ApJ, 447, L95
5. Gezari, D. et al, 1985, ApJ, 299, 1007
6. Ghez, A., Klein, B. L., Morris, M., & Becklin, E. E., 1998, ApJ, 509, 678
7. Stolovy, S., Hayward, T. L., & Herter, T., 1996, ApJ, 470, L45
8. Reid, M., 1993, ARA&A, 31, 345
9. Matthews, K., Ghez, A. M., Weinberger, A. J., & Neugebauer, G., 1996, PASP, 108, 615
10. Matthews, K. & Soifer, B., T., 1994, Astronomy with Infrared Arrays: The Next Generation, ed. I McLean, Klewer Academic Publications (Astrophysics and Space Science, v. 190, p. 239)
11. Ressler, M., E., Werner, M., W., Van Cleve, J., & Choa, H., 1994, Exp. Astron., 3, 277
12. Gezari, D. 1992 in *The Center, Bulge and Disk of the Milky Way*, ed. L. Blitz, (Dordrecht: Kluwer), 23
13. Rowan-Robinson, M., & Harris, S., 1983, MNRAS, 202, 797
14. Tuthill, P., Monnier,J., & Danchi, W., 1999, Nature, 398, 487
15. Danks, A. C., Dennefeld, M., Wamsteker, W., & Shaver, P. A., 1983, A&A, 118, 301
16. Aitken, D. K., Gezari, D., Smith, C. H., McCaughrean, M., & Roche,P. F., 1991, ApJ, 380, 419
17. Becklin, E. E., Matthews, K., Neugebauer, G., & Willner, S. P. 1978, ApJ, 219, 121
18. Sellgren, K., Allamandola, L., Bregman, J., Werner, M., & Wooden, D., 1985, ApJ, 299, 416

19. Tokunaga, A.T., 2000, in Astrophysical Quantities, 4th edition, ed. A. Cox, AIP Press
20. Laor, A., & Draine, B., 1993, ApJ, 402, 441
21. Reike, G., Rieke, M., & Paul, A. E., 1989, ApJ, 336, 752
22. Genzel, R., Hollenbach, D., & Townes, C., 1994, Reports of Progress in Physics, 57, 417
23. Tollestrup, E. V., Capps, R. W., & Becklin, E. E., 1989, AJ, 98, 204
24. DePoy, D. L., & Sharp, N. A., 1991, AJ, 101, 1324
25. Simon, M., et al., 1990, ApJ, 360, 95
26. Simons, D., & Becklin, E., 1996, AJ, 111, 1908